

## Emergence of superhydrophobic behavior on vertically aligned nanocone arrays

B. D'Urso<sup>a)</sup> and J. T. Simpson

Engineering Science and Technology Division, Oak Ridge National Laboratory, Oak Ridge, Tennessee 37831

M. Kalyanaraman

Department of Electrical and Computer Engineering, University of Tennessee, Knoxville, Tennessee 37996

(Received 13 November 2006; accepted 18 December 2006; published online 22 January 2007)

The authors investigate the properties of water drops on uniform arrays of vertically aligned nanocones. A simple model predicts a variety of behaviors depending on the nanocone aspect ratio. At low aspect ratios, surface tension pulls the water into the nanocone array, resulting in a wetted drop with high contact angle hysteresis. At high aspect ratios, the effect of the surface tension is reversed, resulting in little liquid-solid contact and drops which easily slide off the surface. Experiments show that the transition occurs as a gradual change in drop contact angles, but an abrupt change in sliding angles. © 2007 American Institute of Physics. [DOI: 10.1063/1.2433039]

The behavior of water on superhydrophobic surfaces consisting of an array of pillars has been thoroughly studied.<sup>1-3</sup> As the height of the pillars is increased from zero, the drop can either be in a fully wetted (Wenzel) state<sup>4</sup> or it can be suspended on top of the pillars in a composite (Cassie) state.<sup>5</sup> The states are separated by an energy barrier, and often irreversible transitions between the states can be driven by force.<sup>6</sup> Since only the Cassie state has the anti-sticking properties typically associated with superhydrophobicity, design rules have been determined to ensure that it is the dominant state.<sup>7</sup>

We investigate the emergence of superhydrophobicity on ordered, vertically aligned arrays of nanocones. The transition to a superhydrophobic surface as the dominant state changes from the Wenzel state to the Cassie state with increasing aspect ratio is easily observed. A simple model, which provides a clear understanding of the origin of superhydrophobic behavior, predicts the transition from one state to the other.

Consider a single nanocone which is dry except for a small region around the tip which is wetted. We assume that the liquid-solid-vapor line is a circle, i.e., the wetting is circularly symmetric around the cone. Even in an array, this is a reasonable assumption as long as the wetted fraction of the cones is small, so the effect of the neighboring cones can be ignored. Then, the vertical force on the water due to the surface tension (neglecting line tension<sup>8</sup>) can be easily calculated by integrating the force around the liquid-solid-vapor line, giving

$$F = 2\pi\gamma(d \tan \phi)\sin(\theta_0 - 90^\circ - \phi), \quad (1)$$

where  $\gamma$  is the surface tension of the liquid,  $\theta_0$  is the flat surface liquid-solid contact angle,  $\phi$  is the nanocone apex half-angle, and  $d$  is the wetted cone height (see Fig. 1). Thus,  $d \tan \phi$  is the radius of the liquid-solid-vapor circle. Equation (1) shows that the force takes the form of a simple Hooke's law spring, i.e., the restoring force increases linearly with the displacement of the liquid-solid-vapor line  $d$ .

We can rewrite Eq. (1) for an array of nanocones in terms of restoring pressure  $P$  as

$$P = 2\gamma\sqrt{\pi\rho\alpha}\sin\phi\sin(\theta_0 - 90^\circ - \phi), \quad (2)$$

where  $\rho$  is the area density of nanocones and  $\alpha$  is the fraction of wet area relative to the total projected area. The resulting restoring pressure  $P$  is plotted for different  $\theta_0$  and  $\phi$  in Fig. 2. For  $\phi$  near zero (very high aspect ratio), the restoring pressure is low for a given fractional area of contact because of the short length of liquid-solid-vapor line with a fixed  $\alpha$ . For large  $\phi$  (low aspect ratio), the sign of the vertical component of the surface tension force is reversed and the liquid is pulled further into the surface features. The restoring pressure is zero when  $\phi = \theta_0 - 90^\circ$  because the surface tension forces are completely horizontal. The optimal  $\phi$ , which maximizes the restoring pressure, can be found by maximizing Eq. (2); to first order the solution is  $\phi_{\text{opt}} \approx (\theta_0 - 90^\circ)/3$ . This approximation is a reasonable design guide over the typical accessible range of hydrophobic materials, which have  $90^\circ < \theta_0 < 130^\circ$ . Even at the extreme end of this range ( $\theta_0 = 130^\circ$ ), there is acceptable agreement between the linear approximation, which gives  $\phi_{\text{opt}} = 13.3^\circ$ , and the complete solution, which gives  $\phi_{\text{opt}} = 13.8^\circ$ .

We measure the contact and rolling angles of water drops on vertically aligned nanocone arrays based on nanocone array glass<sup>9</sup> with a range of apex angles. Briefly, the nanocones are produced by drawing an acid-resistant glass rod inside a more acid-etchable glass tube into a fiber. The

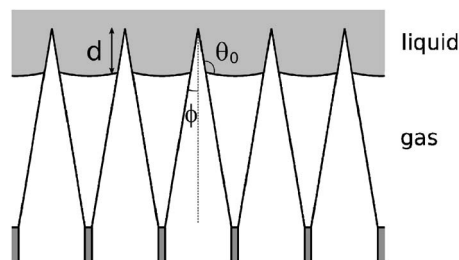


FIG. 1. Cross-sectional diagram of vertically aligned nanocone array showing dimensions and angles used in the model.

<sup>a)</sup>Electronic mail: dursobr@ornl.gov

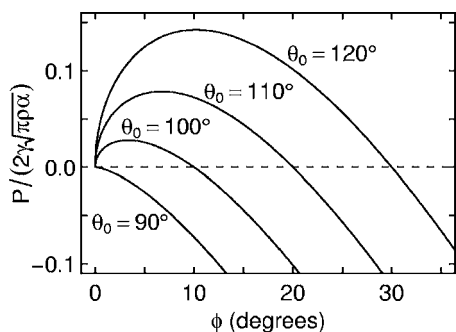


FIG. 2. Plot of the predicted restoring pressure for liquid on a nanocone array with a flat-surface liquid-solid contact angle of  $\theta_0$  and apex half-angle  $\phi$ .

fiber is repeatedly cut into short pieces, bundled into a hexagonal bundle, and drawn into fiber. The resulting fiber is fused into a larger solid bundle, sliced, and etched with a hydrofluoric acid solution to form nanocones with a lattice constant of  $1.6 \mu\text{m}$ . Changes in the etching solution allow the aspect ratio of the nanocones to be varied from 0.4 to 13 (see Fig. 3). To make the surface hydrophobic, the etched surfaces are coated with a fluorinated self-assembled monolayer (SAM).<sup>10</sup> The coating is applied by immersing the samples in a 1% solution of (tridecafluoro-1,1,2,2-tetrahydrooctyl)trichlorosilane in hexane for 30 min. The samples are dried, heated at  $110^\circ\text{C}$  for 15 min, and cleaned in isopropanol with ultrasonic agitation. The samples are allowed to thoroughly dry for at least 24 h before testing.

Contact angles are measured on flat and nanocone surfaces with the hydrophobic SAM coating. A  $10 \mu\text{l}$  drop of distilled water is dispensed from a flat-tipped stainless steel needle onto each surface. The tip is left in contact with the drop during all measurements to prevent the drop from roll-

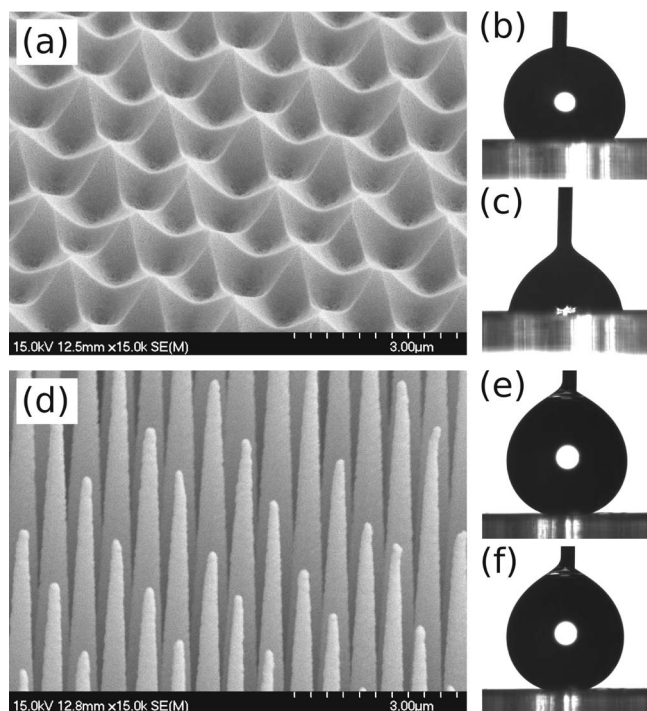


FIG. 3. SEM images of nanocone arrays and optical images of water drops on nanocone arrays. (a) Lowest aspect ratio nanocones tested, with (b) advancing drop and (c) receding drop. (d) Highest aspect ratio nanocones tested, with (e) advancing drop and (f) receding drop.

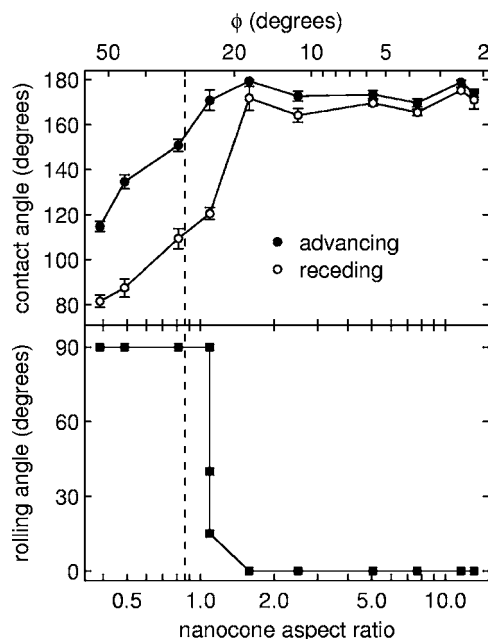


FIG. 4. Plot of results of (top) advancing and receding contact angle and (bottom) rolling angle measurements of water drops on nanocone arrays depending on the nanocone aspect ratio (or apex half-angle  $\phi$ ). The vertical dashed line indicates the location of the predicted Wenzel to Cassie transition. Each contact angle data point and error bar is the mean and standard deviation of the mean of five measurements. For all but one nanocone aspect ratio, the drops would not roll off the surface at any inclination (indicated as  $90^\circ$ ) or could not be balanced on the surface (indicated as  $0^\circ$ ).

ing off the sample. Due to contact angle hysteresis,<sup>11</sup> the contact angle while the drop is growing (the advancing angle) is larger than that when the drop is shrinking (the receding angle). The drop profiles are photographed, and the drop contour is fit with the axisymmetric drop shape analysis method<sup>12</sup> modified to include the needle tip in contact with the drop. The angle at which a  $10 \mu\text{l}$  drop rolls off of the surface is also measured.

Contact angles and rolling angles are measured on nanocone arrays with ten different aspect ratios ranging from 0.4 to 13. The tested structures, along with images of advancing and receding drops on two surfaces are shown in Fig. 3, and all the results are summarized in Fig. 4. For a flat glass surface coated with the SAM, the advancing contact angle  $\theta_{0A} = 120^\circ$  and the receding contact angle  $\theta_{0R} = 90^\circ$ .

For very low nanocone aspect ratios, we have  $\theta_{0A} - 90^\circ < \phi$ , so our model predicts that the forces due to the liquid surface tension are expected to pull water on the nanocone surface further into the spaces between the nanocones until the entire surface is wetted. Our measurements show that the advancing and receding contact angles on the nanocone surface are increased relative to the flat surface, but the contact angle hysteresis ( $\theta_{0A} - \theta_{0R}$ ) is large and the drops do not roll off the surface even when it is held vertically, consistent with the Wenzel (fully wetted) state.

When the nanocone aspect ratio increases, we enter a second regime, where  $\theta_{0R} - 90^\circ < \phi < \theta_{0A} - 90^\circ$ . For the observed  $\theta_{0R}$  and  $\theta_{0A}$ , this occurs for  $0^\circ < \phi < 30^\circ$ . Here, the model predicts that the surface tension forces push the water out of the space between the nanocones, at least when the water is advancing. The result is that a layer of air separates most of the liquid from direct contact with the solid, as the water rests on little more than the tips of the nanocones. We

observe a continued increase in the advancing and receding contact angles as we enter this regime, and a fairly abrupt change in the rolling angle of a drop on the surface. Our model predicts that the transition takes place at  $\phi=30^\circ$ . We observe that  $10\ \mu\text{l}$  drops stick to the surface even if the surface is held vertically with  $\phi\geq 32^\circ$ , but roll off the surface so easily that they cannot be balanced if  $\phi\leq 18^\circ$ . In between, there is one sample which gives inconsistent results: a first drop placed on the surface rolled off, but repeating the test leads to drops that stick. The drops which roll off easily are consistent with the Cassie (composite) state, indicating that the water is pushed out of the space between the nanocones, as expected. We interpret the one data point with inconsistent results as being in a Cassie state initially, but with insufficient restoring force to completely keep the water out from between the nanocones. Once the water penetrates these spaces, contact angle hysteresis holds it in.

For all samples tested, we find that water drops condensed on the surface from vapor stick to the surface, apparently in the Wenzel state, as has also been observed on the lotus leaf.<sup>13</sup> With the appropriate combination of base material and geometry, a third regime could be obtained, with  $\phi < \theta_{0R} - 90^\circ$ . This regime is not accessible here because of the low value of  $\theta_{0R}$ . Water condensed from vapor onto the surface in this regime may be pushed out from between the nanocones and roll off the surface easily. However, as with pillar arrays, there may be an energy barrier which obstructs the transition from the wetted Wenzel state to the composite Cassie state.<sup>6</sup>

As we show, the superhydrophobic behavior of nanocone arrays can be simply modeled, and a transition from a dominant Wenzel to Cassie state is predicted. Measurements of contact angles and rolling angles both confirm the prediction, although contact angle hysteresis softens the transition. The simplicities of the model and system provide insight into the origin of superhydrophobic behavior and the possibility of condensation-repellent superhydrophobic materials.

This Research was sponsored by the Laboratory Directed Research and Development Program of Oak Ridge National Laboratory (ORNL), managed by UT-Battelle, LLC for the U.S. Department of Energy under Contract No. DE-AC05-00OR22725.

<sup>1</sup>Z. Yoshimitsu, A. Nakajima, T. Watanabe, and K. Hashimoto, *Langmuir* **18**, 5818 (2002).

<sup>2</sup>B. He, N. A. Patankar, and J. Lee, *Langmuir* **19**, 4999 (2003).

<sup>3</sup>L. Zhu, Y. Feng, X. Ye, and Z. Zhou, *Sens. Actuators A* **130**, 595 (2006).

<sup>4</sup>R. N. Wenzel, *Ind. Eng. Chem.* **28**, 988 (1936).

<sup>5</sup>A. B. D. Cassie and S. Baxter, *Trans. Faraday Soc.* **40**, 546 (1944).

<sup>6</sup>A. Lafuma and D. Quéré, *Nat. Mater.* **2**, 457 (2003).

<sup>7</sup>A. Marmur, *Langmuir* **19**, 8343 (2003).

<sup>8</sup>B. V. Toshev, D. Platikanov, and A. Scheludko, *Langmuir* **4**, 489 (1988).

<sup>9</sup>B. D'Urso, J. T. Simpson, and M. Kalyanaraman (unpublished).

<sup>10</sup>M. J. Pellerite, E. J. Wood, and V. W. Jones, *J. Phys. Chem. B* **106**, 4746 (2002).

<sup>11</sup>L. Gao and T. J. McCarthy, *Langmuir* **22**, 6234 (2006).

<sup>12</sup>Y. Rotenburg, L. Boruvka, and A. W. Neumann, *J. Colloid Interface Sci.* **93**, 169 (1983).

<sup>13</sup>Y.-T. Cheng and D. E. Rodak, *Appl. Phys. Lett.* **86**, 144101 (2005).